2011

High-order finite difference methods with subcell resolution for 2D detonation waves

W. Wang

C.-W. Shu

Helen Yee

Bjorn Sjögreen

High-order finite difference methods with subcell resolution for 2D detonation waves

By W. Wang†, C.-W. Shu‡, H. C. Yee¶ AND B. Sjögreen‖

1. Motivation and objective

In simulating hyperbolic conservation laws in conjunction with an inhomogeneous stiff source term, if the solution is discontinuous, spurious numerical results may be produced due to the different time scales of the transport part and the source term. This numerical issue often arises in combustion and high-speed chemical reacting flows.

The reactive Euler equations in two dimensions have the form

$$U_t + F(U)_x + G(U)_y = S(U), \tag{1.1}$$

where U, $F(U)$, $G(U)$ and $S(U)$ are vectors. If the time scale of the ordinary differential equation (ODE) $U_t = S(U)$ for the source term is orders of magnitude smaller than the time scale of the homogeneous conservation law $U_t + F(U)_x + G(U)_y = 0$ then the problem is said to be stiff. In high-speed chemical reacting flows, the source term represents the chemical reactions which may be much faster than the gas flow. This leads to problems of numerical stiffness. Insufficient spatial/temporal resolution may cause an incorrect propagation speed of discontinuities and nonphysical states in standard dissipative numerical methods.

This numerical phenomenon was first observed by Colella *et al.* (1986). Then LeVeque & Yee (1990) showed that a similar spurious propagation phenomenon can be observed even with scalar equations. Colella *et al.* (1986) and Majda & Roytburd (1990) have successfully applied the random choice method of Chorin (1976, 1977) for the solution of underresolved detonation waves. However, it is difficult to eliminate completely the numerical viscosity in a shock-capturing scheme. Fractional step methods are commonly used for allowing an underresolved mesh size with a shock-capturing method. Chang (1989, 1991) applied the subcell resolution method of Harten (1989) to the finite volume ENO method in the convection step, which is able to produce a zero viscosity shock profile in nonreacting flow. The time evolution is advanced along the characteristic line. Correct discontinuity speed was obtained in the one-dimensional scalar case. However, it is difficult to extend this approach to multi-dimensions and to system of equations because of the reliance on the exact time evolution via characteristics. Engquist & Sjögreen (1991) proposed a simple temperature extrapolation method based on finite difference ENO schemes with implicit Runge-Kutta time discretization, which uses a first-/second-order extrapolation of the temperatures from outside the shock profile. The method is easy to extend to multi-dimensions. Their method is not a fractional step method. It does not seem to work well when the spatial scales are underresolved. Other first-/second-order

† Department of Mathematics and Statistics, Florida International University, Miami, FL 33199
‡ Division of Applied Mathematics, Brown University, Providence, RI 02912
¶ NASA Ames Research Center, Moffett Field, CA 94035
‖ Lawrence Livermore National Laboratory, Livermore, CA 94551

methods that are based on the fractional step method have been proposed by Bao & Jin (2000, 2001) and Tosatto & Vigevano (2008).

In our previous work by Wang *et al.* (2010), we developed a high-order finite difference method which can capture the correct detonation speed in an underresolved mesh and will maintain high-order accuracy in the smooth part of the flow. Numerical examples were presented for one-dimensional scalar problems and one-dimensional detonation waves. Our objective in this study is to extend this method to two-dimensional reactive Euler equations. The first step of the proposed fractional step method is the convection step which solves the homogeneous hyperbolic conservation law in which any high-resolution shock-capturing method can be used. The aim in this step is to produce a sharp wave front, but some numerical dissipation is allowed. The second step is the reaction step where an ODE solver is applied with modified transition points. Here, by transition points, we refer to the smeared numerical solution in the shock region, which is due to the dissipativity of a shock-capturing scheme. Because the transition points in the convection step will result in large erroneous values of the source term if the source term is stiff, we first identify these points and then extrapolate them by a reconstructed polynomial using the idea of Harten's subcell resolution method. Unlike Chang's approach, we apply Harten's subcell resolution in the reaction step. Thus our approach is flexible in allowing any shock-capturing scheme as the convection operator. In the reaction step, since the extrapolation is based on the high-order reconstruction, high-order accuracy can be achieved in space. The only drawback in our current approach is that the temporal accuracy will only be, at most, second-order due to the time splitting, which is common for most of the previous methods for stiff sources. We also remark that, in order to resolve the sharp reaction zone, sufficiently many grid points in this zone are still needed. The proposed method can capture the correct location and jump size of the reaction front, but it does not resolve the narrow reaction zone, as typically there is one or a few points in that zone.

2. Two-dimensional reactive Euler equations

The considered two-dimensional problem is modeling the reaction with two chemical states: burnt gas and unburnt gas. The unburnt gas is converted to burnt gas via a single irreversible reaction. Without heat conduction and viscosity, the system can be written as

$$\rho_t + (\rho u)_x + (\rho v)_y = 0 \tag{2.1}$$

$$(\rho u)_t + (\rho u^2 + p)_x + (\rho uv)_y = 0 \tag{2.2}$$

$$(\rho v)_t + (\rho uv)_x + (\rho v^2 + p)_y = 0 \tag{2.3}$$

$$E_t + (u(E+p))_x + (v(E+p))_y = 0 \tag{2.4}$$

$$(\rho z)_t + (\rho uz)_x + (\rho vz)_y = -K(T)\rho z, \tag{2.5}$$

where $\rho(x, y, t)$ is the mixture density, $u(x, y, t)$ and $v(x, y, t)$ are the mixture x- and y-velocities, $E(x, y, t)$ is the mixture total energy per unit volume, $p(x, y, t)$ is the pressure, $z(x, y, t)$ is the mass fraction of the unburnt gas, $K(T)$ is the chemical reaction rate and $T(x, y, t)$ is the temperature. The pressure is given by

$$p = (\gamma - 1)(E - \frac{1}{2}\rho(u^2 + v^2) - q_0\rho z), \tag{2.6}$$

where the temperature $T = \frac{p}{\rho}$ and q_0 is the heat released in the reaction.

The reaction rate $K(T)$ is modeled by an Arrhenius law

$$K(T) = K_0 \exp\left(\frac{-T_{ign}}{T}\right), \tag{2.7}$$

where K_0 is the reaction rate constant and T_{ign} is the ignition temperature. The reaction rate may be also modeled in the Heaviside form

$$K(T) = \begin{cases} 1/\varepsilon & T \geq T_{ign} \\ 0 & T < T_{ign} \end{cases}, \tag{2.8}$$

where ε is the reaction time and $1/\varepsilon$ is roughly equal to K_0. For simplicity, we only consider the Heaviside source term (2.8).

3. Numerical method for two-dimensional reactive Euler equations

The general fractional step approach based on Strang-splitting (Strang 1968) for equation

$$U_t + F(U)_x + G(U)_y = S(U) \tag{3.1}$$

is as follows. The numerical solution at time level t_{n+1} is approximated by

$$U^{n+1} = A\left(\frac{\Delta t}{2}\right) R(\Delta t) A\left(\frac{\Delta t}{2}\right) U^n. \tag{3.2}$$

The convection operator A is defined to approximate the solution of the homogeneous part of the problem on the time interval, i.e.,

$$U_t + F(U)_x + G(U)_y = 0, \quad t_n \leq t \leq t_{n+1}. \tag{3.3}$$

The reaction operator R is defined to approximate the solution on a time step of the reaction problem:

$$\frac{dU}{dt} = S(U), \quad t_n \leq t \leq t_{n+1}. \tag{3.4}$$

The convection operator is over a time step Δt and the reaction operator is over $\Delta t/2$. The two half-step reaction operations over adjacent time steps can be combined to save cost.

Next, we introduce the proposed fractional step methods for the convection step and the reaction step separately.

3.1. *Convection operator*

In the convection step, we use fifth-order WENO (WENO5) with Lax-Friedrichs flux and third-order Runge-Kutta for time discretization.

3.2. *Reaction operator*

If there is no smearing of discontinuities in the convection step, any ODE solver can be used as the reaction operator. However, all the standard shock-capturing schemes will produce a few transition points in the shock when solving the convection equation. These transition points are usually responsible for causing incorrect numerical results in the stiff case. Thus we cannot directly apply a standard ODE solver at these transition points.

Here we use Harten's subcell resolution technique in the reaction step. The general idea is as follows. If a point is considered a transition point of the shock, information from its neighboring points which are deemed non-transitional points will be used instead.

In the two-dimensional case, we apply the subcell resolution procedure dimension by dimension.

(1) Use a "shock indicator" to identify cells in which discontinuities are believed to be situated. We consider the minmod-based shock indicator in Harten (1989) and Shu & Osher (1989). Identify troubled cell I_{ij} in both x- and y-directions by applying the shock indicator to the mass fraction z.

Define the cell I_{ij} as troubled in the x-direction if $|s^x_{ij}| \geq |s^x_{i-1,j}|$ and $|s^x_{ij}| \geq |s^x_{i+1,j}|$ with at least one strict inequality where

$$s^x_{ij} = \text{minmod}\{z_{i+1,j} - z_{ij}, z_{ij} - z_{i-1,j}\}. \tag{3.5}$$

Similarly, we can define the cell I_{ij} as troubled in the y-direction if $|s^y_{ij}| \geq |s^y_{i,j-1}|$ and $|s^y_{ij}| \geq |s^y_{i,j+1}|$ with at least one strict inequality where

$$s^y_{ij} = \text{minmod}\{z_{i,j+1} - z_{ij}, z_{ij} - z_{i,j-1}\}. \tag{3.6}$$

If I_{ij} is troubled in only one direction, we apply the subcell resolution along this direction. If I_{ij} is troubled in both directions, we choose the direction which has a larger jump. Namely, if $|s^x_{ij}| \geq |s^y_{ij}|$, subcell resolution is applied along the x-direction, otherwise it is done along the y-direction.

In the following steps (2)-(3), without loss of generality, we assume the subcell resolution is applied in the x-direction.

(2) In a troubled cell identified above, we continue to identify its neighboring cells. For example, we can define $I_{i+1,j}$ as troubled if $|s^x_{i+1,j}| \geq |s^x_{i-1,j}|$ and $|s^x_{i+1,j}| \geq |s^x_{i+2,j}|$ and similarly define $I_{i-1,j}$ as troubled if $|s^x_{i-1,j}| \geq |s^x_{i-2,j}|$ and $|s^x_{i-1,j}| \geq |s^x_{i+1,j}|$. If the cell $I_{i-s,j}$ and the cell $I_{i+r,j}$ $(s, r > 0)$ are the first good cells from the left and the right (i.e., $I_{i-s+1,j}$ and $I_{i+r-1,j}$ are still troubled cells), we compute the fifth-order ENO interpolation polynomial $p_{i-s,j}(x)$ and $p_{i+r,j}(x)$ for the cells $I_{i-s,j}$ and $I_{i+r,j}$, respectively.

Modify the point values z_{ij}, T_{ij} and ρ_{ij} in the troubled cell I_{ij} by the ENO interpolation polynomials

$$\begin{cases} \tilde{z}_{ij} = p_{i-s,j}(x_i; z), \quad \tilde{T}_{ij} = p_{i-s,j}(x_i; T), \quad \tilde{\rho}_{ij} = p_{i-s,j}(x_i; \rho), & \text{if } \theta \geq x_i \\ \tilde{z}_{ij} = p_{i+r,j}(x_i; z), \quad \tilde{T}_{ij} = p_{i+r,j}(x_i; T), \quad \tilde{\rho}_{ij} = p_{i+r,j}(x_i; \rho), & \text{if } \theta < x_i \end{cases}, \tag{3.7}$$

where the location θ is determined by the conservation of energy E

$$\int_{x_{i-1/2}}^{\theta} p_{i-s,j}(x; E)dx + \int_{\theta}^{x_{i+1/2}} p_{i+r,j}(x; E)dx = E_{ij}\Delta x. \tag{3.8}$$

Under certain conditions, it can be shown that there is a unique θ satisfying Eq. (3.8), which can be solved using, for example, Newton's method. If there is no solution for θ or more than one solution, we choose $\tilde{z}_{ij} = z_{i+r,j}$, $\tilde{T}_{ij} = T_{i+r,j}$ and$\tilde{\rho}_{ij} = \rho_{i+r,j}$. However, in the system case we would like to have the shock travel ahead of the reaction zone, so we take the values of z, T and ρ ahead of the shock.

For simplicity, in the considered stiff problem, the value of z_{ij} can be taken as

$$\tilde{z}_{ij} = \begin{cases} 0, & \theta \geq x_i \\ 1, & \theta < x_i \end{cases}. \tag{3.9}$$

(3) Use $\tilde{U}_{ij}$ instead of U_{ij} in the ODE solver if the cell I_{ij} is a troubled cell.

For simplicity, explicit Euler is used as the ODE solver.

$$(\rho z)^{n+1}_{ij} = (\rho z)^n_{ij} + \Delta t S(\tilde{T}_{ij}, \tilde{\rho}_{ij}, \tilde{z}_{ij}). \tag{3.10}$$

Here implicit methods cannot be used in this step because the troubled values need to be modified explicitly. However, there is no small time-step restriction in the explicit method used here, because once the stiff points have been modified, the modified source term $S(\tilde{T}_{ij}, \tilde{\rho}_{ij}, \tilde{z}_{ij})$ is no longer stiff. Therefore, a regular CFL number is allowed in the explicit method.

In general, a regular CFL=0.1 can be used in the proposed scheme to produce a stable solution. But the solution is very coarse in the reaction zone because of the underresolved mesh in time. In order to obtain more accurate results in the reaction zone, we evolve one reaction step via N_r sub steps, i.e.,

$$u^{n+1} = A\left(\frac{\Delta t}{2}\right) R\left(\frac{\Delta t}{N_r}\right) \cdots R\left(\frac{\Delta t}{N_r}\right) A\left(\frac{\Delta t}{2}\right) u^n \tag{3.11}$$

in some numerical examples.

3.3. *A numerical example of 2D detonation waves*

This example is taken from Bao & Jin (2000). The chemical reaction is modeled by the Heaviside form with the parameters

$$\gamma = 1.4, \quad q_0 = 0.5196 \times 10^{10}, \quad \frac{1}{\varepsilon} = 0.5825 \times 10^{10}, \quad T_{ign} = 0.1155 \times 10^{10}$$

in CGS units.

Consider a two-dimensional channel of width 0.005, and the upper and lower boundaries are solid walls. The computational domain is $[0, 0.025] \times [0, 0.005]$. The initial conditions are

$$(\rho, u, v, p, z) = \begin{cases} (\rho_l, u_l, 0, p_l, 0), & \text{if } x \le \xi(y), \\ (\rho_r, u_r, 0, p_r, 1), & \text{if } x > \xi(y), \end{cases} \tag{3.12}$$

where

$$\xi(y) = \begin{cases} 0.004 & |y - 0.0025| \ge 0.001, \\ 0.005 - |y - 0.0025| & |y - 0.0025| < 0.001, \end{cases} \tag{3.13}$$

and $u_l = 8.162 \times 10^4$, $\rho_l = 1.201 \times 10^{-3}$ and $p_l = 8.321 \times 10^5$.

Similar problems are also computed in Engquist & Sjögreen (1991). One important feature of this solution is the appearance of triple points, which travel in the transverse direction and reflect from the upper and lower walls. The mechanisms driving this solution are discussed in Kailasanath *et al.* (1985).

Figures 1-2 show density contours computed by WENO5/SR with 500×100 ($\Delta x = \Delta y = 5 \times 10^{-5}$), CFL=0.1 and $N_r = 2$ at eighteen evolutionary times from $t = 0$ to $t = 1.7 \times 10^{-7}$. We can see the movement of the triple points. The same case by WENO5/SR with a much coarser grid 200×40 ($\Delta x = \Delta y = 1.25 \times 10^{-4}$) with CFL=0.1 and $N_r = 2$ at three evolutionary times is shown in Figure 3. We can see WENO5/SR with the very coarse 200×40 mesh can still capture the correct shock location, although the shocks are smeared due to the lack of resolution. It is more apparent to compare the computed results with the reference solution in a 1D cross section. The reference solutions are computed by standard WENO5 with 2000×400 grid points and CFL=0.3. The results by WENO5/SR and the splitting WENO5 are compared with the same mesh 200×40 and CFL=0.005. Figures 4-7 show the 1D cross section at $y = 0.0025$ at evolutionary times $t = 2 \times 10^{-8}$, $t = 6 \times 10^{-8}$, $t = 1.4 \times 10^{-7}$ and $t = 1.7 \times 10^{-7}$ separately, where the left subplots are computed by WENO5/SR and the right subplots are by splitting WENO5. We can see WENO5/SR has excellent agreement with the reference solutions

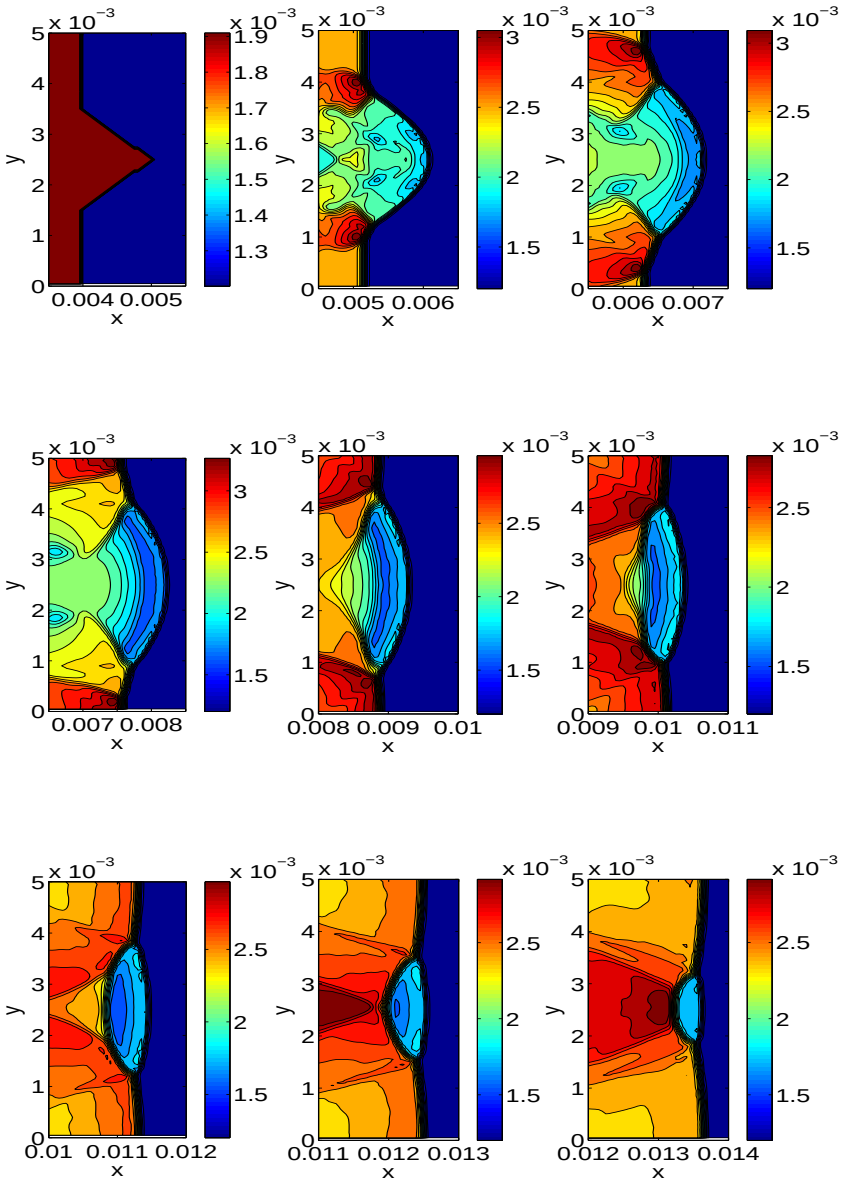

FIGURE 1. Computed density: WENO5/SR with 500×100, CFL=0.1 and $N_r = 2$ at nine different evolutionary times $t = 0$, $t = 1 \times 10^{-8}$, $t = 2 \times 10^{-8}$, $t = 3 \times 10^{-8}$, $t = 4 \times 10^{-8}$, $t = 5 \times 10^{-8}$, $t = 6 \times 10^{-8}$, $t = 7 \times 10^{-8}$ and $t = 8 \times 10^{-8}$.

except that it cannot capture the waves sharply due to the underresolved mesh. However, the splitting WENO5 method produces spurious waves in front of the detonation shock starting at time $t = 2 \times 10^{-8}$ (right subplot of Figure 4) and after that the solutions move at a wrong speed (right subplots of Figures 5-7).

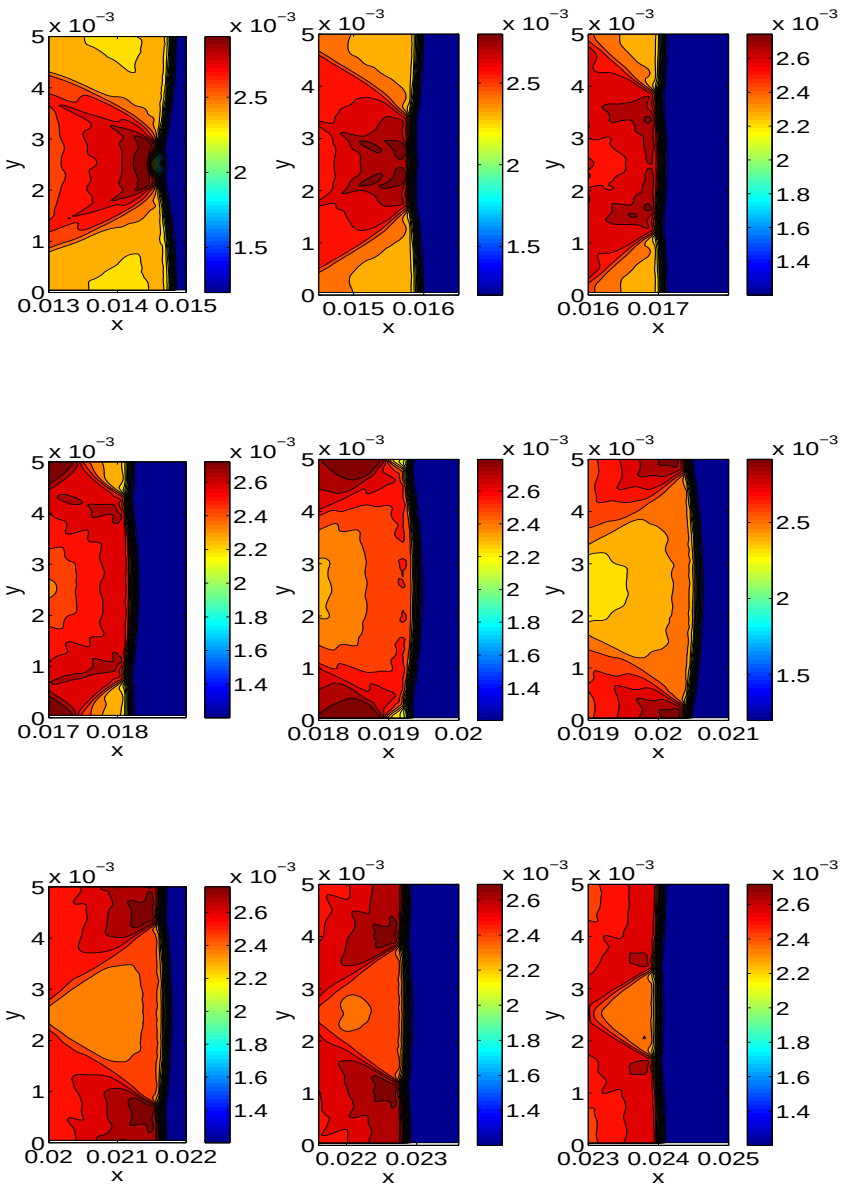

FIGURE 2. Computed density: WENO5/SR with 500×100, CFL=0.1 and $N_r = 2$ at nine different evolutionary times $t = 9 \times 10^{-8}$, $t = 1 \times 10^{-7}$, $t = 1.1 \times 10^{-7}$, $t = 1.2 \times 10^{-7}$, $t = 1.3 \times 10^{-7}$, $t = 1.4 \times 10^{-7}$, $t = 1.5 \times 10^{-7}$, $t = 1.6 \times 10^{-7}$ and $t = 1.7 \times 10^{-7}$.

4. Future plans

In this report, we demonstrated that the proposed high-order finite difference schemes with subcell resolution are able to capture the correct detonation wave speed in two-

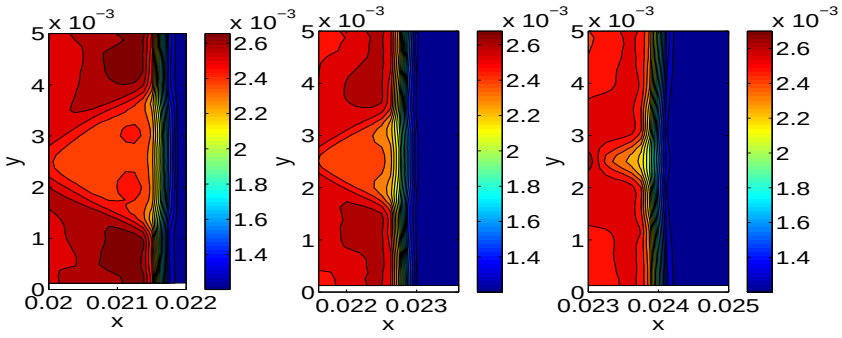

FIGURE 3. Computed results: WENO5/SR with 200×40, CFL=0.1 and $N_r = 2$ at $t = 1.5 \times 10^{-7}$, $t = 1.6 \times 10^{-7}$ and $t = 1.7 \times 10^{-7}$.

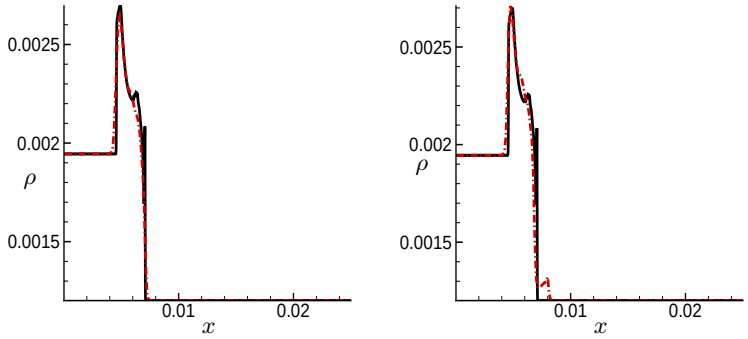

FIGURE 4. 1D cross-section at $t = 2 \times 10^{-8}$ by different WENO schemes with 200×40. Solid line: reference solution; dashed line: numerical solution. Left: WENO5/SR with CFL=0.1, $N_r = 2$; right: splitting WENO5 with CFL=0.05.

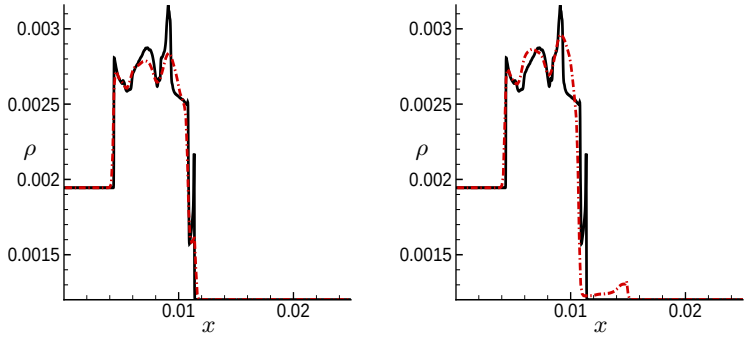

FIGURE 5. 1D cross-section at $t = 6 \times 10^{-8}$ by different WENO schemes with 200×40. Solid line: reference solution; dashed line: numerical solution. Left: WENO5/SR with CFL=0.1, $N_r = 2$; right: splitting WENO5 with CFL=0.05.

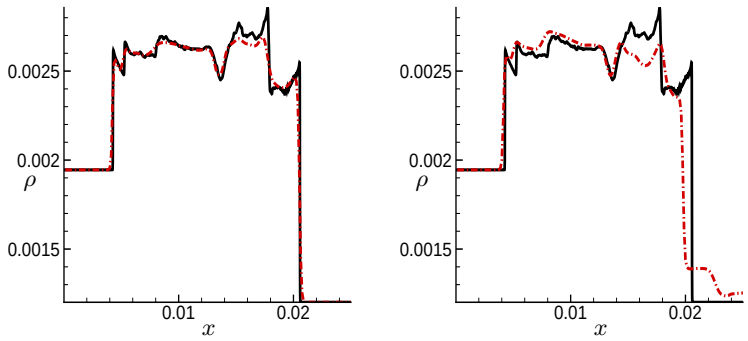

FIGURE 6. 1D cross-section at $t = 1.4 \times 10^{-7}$ by different WENO schemes with 200×40. Solid line: reference solution; dashed line: numerical solution. Left: WENO5/SR with CFL=0.1, $N_r = 2$; right: splitting WENO5 with CFL=0.05.

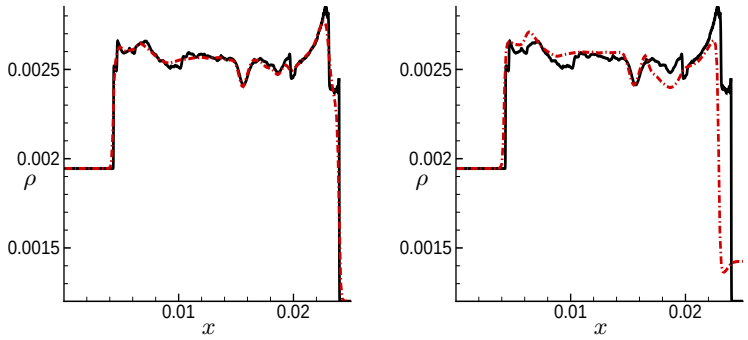

FIGURE 7. 1D cross-section at $t = 1.7 \times 10^{-7}$ by different WENO schemes with 200×40. Solid line: reference solution; dashed line: numerical solution. Left: WENO5/SR with CFL=0.1, $N_r = 2$; right: splitting WENO5 with CFL=0.05.

dimensional system cases. Future work will extend this approach to multiple reaction models.

Acknowledgments

The authors acknowledge the support of the DOE/SciDAC SAP grant DE-AI02-06ER25796. The work by Björn Sjögreen was performed under the auspices of the U.S. Department of Energy at Lawrence Livermore National Laboratory under Contract DE-AC52-07NA27344. The research of C.-W. Shu is also partially supported by ARO grant W911NF-08-1-0520. The research of H. C. Yee is also partially supported by the NASA Fundamental Aeronautics Hypersonic program.

REFERENCES

BAO, W. & JIN, S. 2000 The random projection method for hyperbolic conservation laws with stiff reaction terms. *J. Comp. Phys.* **163**, 216–248.

Bao, W. & Jin, S. 2001 The random projection method for stiff detonation capturing. *J. Sci. Comput.* **23**, 1000–1025.

Chang, S.-H. 1989 On the application of subcell resolution to conservation laws with stiff source terms. *NASA Technical Memorandum 102384, ICOMP Report 89-27* .

Chang, S.-H. 1991 On the application of subcell resolution to conservation laws with stiff source terms. *NASA Lewis Research Center, Computational Fluid Dynamics Symposium on Aeropropulsion* pp. 215–225.

Chorin, A. 1976 Random choice solution of hyperbolic systems. *J. Comp. Phys.* **22**, 517–533.

Chorin, A. 1977 Random choice methods with applications for reacting gas flows. *J. Comp. Phys.* **25**, 253–272.

Colella, P., Majda, A. & Roytburd, V. 1986 Theoretical and numerical structure for numerical reacting waves. *SIAM J. Sci. STAT. Comp.* **7**, 1059–1080.

Engquist, B. & Sjögreen, B. 1991 Robust difference approximations of stiff inviscid detonation waves. *Technical Report CAM 91-03, UCLA.* .

Harten, A. 1989 ENO schemes with subcell resolution. *J. Comp. Phys.* **83**, 148–184.

Kailasanath, K., Oran, E. S., Boris, J. P. & Young, T. R. 1985 Determination of detonation cell size and the role of transverse waves in two-dimensional detonations. *Combust. Flame* **61**, 199–209.

LeVeque, R. J. & Yee, H. C. 1990 A study of numerical methods for hyperbolic conservation laws with stiff source terms. *J. Comp. Phys.* **86**, 187–210.

Majda, A. & Roytburd, V. 1990 Numerical study of the mechanisms for initiation of reacting shock waves. *SIAM J. Sci. STAT. Comp.* **11**, 950–974.

Shu, C.-W. & Osher, S. 1989 Efficient implementation of essentially non-oscillatory shock capturing schemes, ii. *J. Comp. Phys.* **83**, 32–78.

Strang, G. 1968 On the construction and comparison of difference schemes. *SIAM J. Numer. Anal.* **5**, 506–517.

Tosatto, L. & Vigevano, L. 2008 Numerical solution of under-resolved detonations. *J. Comp. Phys.* **227**, 2317–2343.

Wang, W., Shu, C.-W., Yee, H. C. & Sjögreen, B. 2010 High-order finite difference methods with subcell resolution for hyperbolic conservation laws with stiff reaction terms: preliminary results. *Annu. Res. Briefs, Center for Turbulence Research, Stanford University* pp. 149–160.